

A COMPARISON OF COARSE SPACES FOR HELMHOLTZ PROBLEMS IN THE HIGH FREQUENCY REGIME*

N. BOOTLAND[†], V. DOLEAN[‡], P. JOLIVET[§], AND P.-H. TOURNIER[¶]

Abstract. Solving time-harmonic wave propagation problems in the frequency domain and within heterogeneous media brings many mathematical and computational challenges, especially in the high frequency regime. We will focus here on computational challenges and try to identify the best algorithm and numerical strategy for a few well-known benchmark cases arising in applications. The aim is to cover, through numerical experimentation and consideration of the best implementation strategies, the main two-level domain decomposition methods developed in recent years for the Helmholtz equation. The theory for these methods is either out of reach with standard mathematical tools or does not cover all cases of practical interest. More precisely, we will focus on the comparison of three coarse spaces that yield two-level methods: the grid coarse space, DtN coarse space, and GenEO coarse space. We will show that they display different pros and cons, and properties depending on the problem and particular numerical setting.

Key words. Helmholtz equations, domain decomposition methods, two-level methods, coarse spaces, high frequency

AMS subject classifications. 65N55, 65N35, 65F10

1. Introduction. This work is motivated by the computational challenges that arise in frequency domain simulations of wave propagation and scattering problems in heterogeneous media. Such problems appear in a broad range of engineering applications, including acoustics, electromagnetics, and seismic inversion.

The discretisation of models describing frequency domain wave problems using finite element methodology typically results in large, indefinite, and ill-conditioned linear systems. These linear systems are difficult to solve using standard methods, particularly for high frequencies and in the presence of complex heterogeneities. In order to maintain accuracy, the number of grid points must grow as a function of the frequency in such a way that, for high frequency problems, the size of the linear systems to be solved becomes prohibitive for direct methods. In such a regime, carefully designed iterative methods are required. Here, we consider a two-level domain decomposition approach for the robust parallel solution of the linear systems.

To model the wave problem we utilise the Helmholtz equation on a domain $\Omega \subset \mathbb{R}^d$, $d = 2, 3$, for the field $u(\mathbf{x}): \Omega \rightarrow \mathbb{C}$ given by

$$(1.1a) \quad -\Delta u - k^2 u = f \quad \text{in } \Omega,$$

$$(1.1b) \quad \mathcal{C}(u) = 0 \quad \text{on } \partial\Omega,$$

where \mathcal{C} incorporates some appropriate boundary conditions, $k(\mathbf{x}) > 0$ is the wave number, and $f(\mathbf{x})$ is a suitable forcing function. A key parameter is the wave number k , which relates the angular frequency ω and the wave speed c as $k = \omega/c$. The wave speed $c(\mathbf{x})$ depends on the position \mathbf{x} in the media for heterogeneous problems. Since

*The first two authors gratefully acknowledge support from the EPSRC grant EP/S004017/1. The fourth author gratefully acknowledges support from the EPSRC grant EP/R009821/1.

[†]Department of Mathematics and Statistics, University of Strathclyde, Glasgow, UK (niall.bootland@strath.ac.uk).

[‡]Department of Mathematics and Statistics, University of Strathclyde, Glasgow, UK and Laboratoire J.A. Dieudonné, CNRS, University Côte d'Azur, Nice, France (work@victoritadolean.com).

[§]IRIT, University of Toulouse, France (pierre.jolivet@enseeiht.fr).

[¶]LJLL, Sorbonne University, France (tournier@ljl.math.upmc.fr).

k is proportional to the frequency, the high frequency regime constitutes the case of large k and presents particular challenges for designing effective solvers.

The difficulty in designing a good solver for the Helmholtz equation is shown very clearly in the review papers [16, 21] where one can see that there are no straightforward extensions to state-of-the-art methods for symmetric positive definite problems that tackle the indefinite or non-self adjoint problem well. When the problems are large, however,—the case when one discretises the Helmholtz equation accurately for high wave numbers—domain decomposition methods are a natural choice [11]. Nevertheless, despite recent efforts and in view of the latest results obtained both at the theoretical [25, 26, 22] or numerical level [12, 13, 32], there is no established method outperforming all others in the case of the Helmholtz problem.

Domain decomposition methods are well suited to solve large systems of equations arising from discretisation of PDEs and are among the best known strategies for many types of problem. However, classical versions fail to be effective and may diverge for wave propagation problems. Two key constituent parts require a more careful treatment: the transmission conditions used to transfer information between adjoining subdomains and the coarse space that allows for capturing of global behaviour and passing information between subdomains globally. In this work we consider overlapping Schwarz methods.

The use of different transmission conditions at the interfaces (artificial boundaries arising from the decomposition into subdomains) has been extensively studied over the past two decades and various works [8, 9, 20] show that these conditions can improve the convergence of Schwarz methods and preconditioners. However, good transmission conditions are not sufficient to ensure a robust behaviour with respect to heterogeneities in the problem to solve or when the number of subdomains increases. To tackle these difficulties we need coarse information that is cheap to compute and immediately available to all subdomains.

The focus in this work is on appropriate coarse spaces. A coarse space is typically required to provide scalability with respect to the number of subdomains used. More recently, however, coarse spaces have been designed to provide robustness to model parameters, especially for large contrasts in complex heterogeneous problems. For example, the GenEO (Generalised Eigenproblems in the Overlap) coarse space has been successfully employed for the robust solution of highly heterogeneous elliptic problems [39, 27]. For the Helmholtz equation, finding a suitable coarse space is not an easy task and, being an indefinite problem, choosing a larger coarse space need not improve performance [19]. In designing coarse spaces for Helmholtz problems we might also wish to reduce the dependence of the domain decomposition method on the wave number k . A natural idea to capture global behaviour is to use plane waves as a basis for the coarse space but it is not clear that this is suitable for heterogeneous media. Plane waves were first used within the multigrid approach [7] before later being used to build coarse spaces for domain decomposition methods. We can cite the example of FETI(-DP)-H methods [18, 17] but they have also been used in other domain decomposition methods [33]. Nonetheless, plane waves have mainly been employed for homogeneous problems and do not have a straightforward extension to the heterogeneous case.

Even if coarse space information needs to be global and available to all domains, coarse spaces can be built locally and based on local functions. Spectral coarse spaces use basis vectors deriving from the solution of local eigenvalue problems associated with appropriate operators. Within the context of the Helmholtz equation, this is exemplified in the DtN coarse space [10]. Here, eigenproblems are formulated on

subdomain interfaces based on a Dirichlet-to-Neumann (DtN) map, extending an approach for elliptic problems [36, 14]. In this work we consider two spectral coarse spaces, the DtN approach and a GenEO-type approach suited to the Helmholtz problem. We will also consider a grid coarse space approach which utilises the addition of absorption in the problem.

Our consideration of coarse spaces for Helmholtz problems in the high frequency regime provide the following main contributions of the paper:

- We bring together and outline recent work on developing coarse spaces that can be utilised to enhance domain decomposition methods for the Helmholtz problem in heterogeneous media. These approaches are then implemented in a common software, namely **FreeFem**.
- We discuss implementation details and practical aspects of the methods as well as contrasting the benefits and drawbacks.
- We provide extensive numerical results on several well-known benchmark problems in 2D and 3D and compare the different approaches within a variety of settings.
- Based on the results of our numerical tests and our understanding of the implementation aspects involved, we provide an outlook on scenarios where certain methods may be more, or less, favourable.

The outline for the remainder of this work is as follows. In [Section 2](#) we detail the boundary value problem considered, i.e. the heterogeneous Helmholtz problem and its discretisation by finite elements. In [Section 3](#) we introduce the basic principles of domain decomposition methods and present two versions of the one-level method, namely RAS and ORAS. A second level, or coarse space, is usually added by deflation. The three different coarse space strategies, namely the grid coarse space, DtN coarse space, and GenEO coarse space, are introduced in [Section 4](#). Parallel implementation details of these methods are given in [Section 5](#) and an extensive numerical study is shown in [Section 6](#). Conclusions are then given in [Section 7](#).

2. The heterogeneous Helmholtz problem. Our model problem consists of solving the interior Helmholtz equation (1.1). To be concrete, we let Ω is a bounded polygonal domain and consider specific boundary conditions on $\Gamma = \partial\Omega$. We suppose Γ is partitioned into a disjoint union $\Gamma = \Gamma_D \cup \Gamma_N \cup \Gamma_R$ where Dirichlet conditions are imposed on Γ_D , Neumann conditions on Γ_N and a Robin condition on Γ_R . Namely, we wish to solve

$$\begin{aligned}
 (2.1a) \quad & -\Delta u - k^2 u = f && \text{in } \Omega, \\
 (2.1b) \quad & u = u_{\Gamma_D} && \text{on } \Gamma_D, \\
 (2.1c) \quad & \frac{\partial u}{\partial \mathbf{n}} = 0 && \text{on } \Gamma_N, \\
 (2.1d) \quad & \frac{\partial u}{\partial \mathbf{n}} + iku = 0 && \text{on } \Gamma_R,
 \end{aligned}$$

where u_{Γ_D} is known. The Robin condition in (2.1d) is a standard first order approximation to the far field Sommerfeld radiation condition and, in essence, enables appropriate wave behaviour to be described in a bounded domain, allowing for incoming or outgoing waves along Ω_R . We do not require that a problem instance includes all types of boundaries but note that if $\Gamma_R = \emptyset$ then the problem will be ill-posed for certain choices of k . Furthermore, when $\Gamma_R \neq \emptyset$ the resulting linear systems, while being complex symmetric, are not Hermitian and this will be important in our choice of iterative method. However, classical iterative methods on their own are not enough

to be able to solve Helmholtz problems effectively [16]. This is further amplified when applied to highly heterogeneous problems.

The heterogeneity in our model is present in the wave number $k(\mathbf{x}) > 0$, being given by ratio of the angular frequency ω and the wave speed $c(\mathbf{x})$ as $k = \omega/c$. We allow k to have jumps across different media and otherwise vary within the domain Ω such that $k \in L^\infty(\Omega)$.

To discretise (2.1) we use the finite element method. In order to prescribe the weak formulation we let $V = \{u \in H^1(\Omega) : u = u_{\Gamma_D} \text{ on } \Gamma_D\}$ and, in a similar fashion, $V_0 = \{u \in H^1(\Omega) : u = 0 \text{ on } \Gamma_D\}$. The weak form of the problem is then to find $u \in V$ such that

$$(2.2) \quad a(u, v) = F(v) \quad \forall v \in V_0,$$

where

$$(2.3a) \quad a(u, v) = \int_{\Omega} (\nabla u \cdot \nabla \bar{v} - k^2 u \bar{v}) \, d\mathbf{x} + \int_{\Gamma_R} iku\bar{v} \, ds,$$

and

$$(2.3b) \quad F(v) = \int_{\Omega} f\bar{v} \, d\mathbf{x},$$

are the bilinear and linear parts, respectively. To discretise we consider piecewise polynomial finite element approximation on a simplicial mesh \mathcal{T}^h of Ω which has a characteristic element diameter h . Denoting the associated trial space $V^h \subset V$ and test space $V_0^h \subset V_0$ the discrete problem is to find $u_h \in V^h$ such that

$$(2.4) \quad a(u_h, v_h) = F(v_h) \quad \forall v_h \in V_0^h.$$

Let $\{\phi_j\}_{j=1}^n$ be the nodal basis for V_0 and $\{\phi_j\}_{j=n+1}^{n+d}$ be the nodal basis for the Dirichlet boundary Γ_D , for which \mathcal{T}^h is assumed to conform. Then we can rewrite (2.4) as a (complex) linear system

$$(2.5) \quad \mathbf{A}\mathbf{u} = \mathbf{f},$$

where the coefficient matrix $A \in \mathbb{C}^{n \times n}$ and right-hand side vector $\mathbf{f} \in \mathbb{C}^n$ are given by $A_{i,j} = a(\phi_j, \phi_i)$ and $f_i = F(\phi_i) - \sum_{l=n+1}^{n+d} a(\phi_l, \phi_i) \bar{u}_{l-n}$ respectively, for $i, j \in 1, 2, \dots, n$. Here \bar{u}_j , for $j = 1, 2, \dots, d$, are the known Dirichlet values along Γ_D corresponding to u_{Γ_D} . We then seek the solution $\mathbf{u} \in \mathbb{C}^n$ of the (in general) complex symmetric indefinite system (2.5) to give

$$(2.6) \quad u_h(\mathbf{x}) = \sum_{j=1}^n u_j \phi_j(\mathbf{x}) + \sum_{l=n+1}^{n+d} \bar{u}_{l-n} \phi_l(\mathbf{x}).$$

The wave nature of solutions to the Helmholtz equation requires a sufficiently fine mesh in order to obtain a good approximation to the true solution and this should be kept in mind when considering the choice of discretisation of the problem. In terms of increasing the wave number k , if one is to maintain the same level of accuracy of discrete solutions then the number of grid points must increase faster than k increases, due to the pollution effect [2]. This growth depends on the discretisation chosen. For instance, in the case of using a piecewise linear (P1) finite element approximation

on simplicial elements of diameter h , then $k^3 h^2$ must be bounded, requiring h to shrink as $\mathcal{O}(k^{-3/2})$. For piecewise quadratic (P2) finite elements on simplicial meshes the criteria relaxes to require that h decreases as $\mathcal{O}(k^{-5/4})$. For higher order finite elements the requirement becomes less stringent but the interpolation properties when using such approximation spaces ultimately begin to degrade.

Due to these restrictions and the desire for faster simulation times, it is common that practitioners simply consider a fixed number of points per wavelength instead, resulting in h decreasing as $\mathcal{O}(k^{-1})$. Given a fixed number, n_{ppwl} , of points per wavelength we ensure that $n_{\text{ppwl}} h \approx \lambda$, where the wavelength is given by $\lambda = 2\pi k^{-1}$. A prevalent engineering practice is to use 10 points per wavelength and in some large real-world problems of interest, such as in imaging science, it may be adequate or necessary to insist on less resolution. In light of this, we consider both 5 and 10 points per wavelength scenarios and make use of standard P2 finite element approximation throughout this work.

3. Domain decomposition. We now give details of the overlapping domain decomposition approach that we will utilise. This will be applied as a preconditioner rather than a stand-alone iterative method. Our approach is based on a two-level version of the optimised restricted additive Schwarz (ORAS) method. To provide a domain decomposition, we first partition Ω into non-overlapping subdomains $\{\Omega'_s\}_{s=1}^N$ which are resolved by the mesh \mathcal{T}^h . A layer of adjoining mesh elements are then added to provide overlapping subdomains $\{\Omega_s\}_{s=1}^N$ through the extension

$$(3.1) \quad \Omega_s = \text{Int} \left(\bigcup_{\text{supp}(\phi_j) \cap \Omega'_s \neq \emptyset} \text{supp}(\phi_j) \right),$$

where $\text{Int}(\cdot)$ denotes the interior of a domain and $\text{supp}(\cdot)$ the support of a function. Note that more than one layer of elements can be added in a recursive manner if subdomains with larger overlap are required.

Now that we have a domain decomposition, we can define the restriction to a given subdomain Ω_s as an operator from V^h into $V^h(\Omega_s) = \{v|_{\Omega_s} : v \in V^h\}$, namely $\mathcal{R}_s : V^h \rightarrow V^h(\Omega_s)$ where $\mathcal{R}_s v = v|_{\Omega_s}$. Let $R_s \in \mathbb{R}^{n_s \times n}$ be the matrix form of \mathcal{R}_s where n_s is the number of degrees of freedom in Ω_s . Since our subdomains overlap, we also make use of a partition of unity having matrix form $D_s \in \mathbb{R}^{n_s \times n_s}$ which is diagonal and satisfies $\sum_{s=1}^N R_s^T D_s R_s = I$; this removes ‘‘double counting’’ in the additive Schwarz method. Note that R_s^T acts as an extension by zero outside of Ω_s .

We can now define the restricted additive Schwarz (RAS) preconditioner

$$(3.2) \quad M_{\text{RAS}}^{-1} = \sum_{s=1}^N R_s^T D_s A_s^{-1} R_s,$$

where $A_s = R_s A R_s^T$ is the local Dirichlet matrix on Ω_s , that is, Dirichlet conditions are implicitly assumed on $\partial\Omega_s \setminus \partial\Omega$. This corresponds to using Dirichlet transmission conditions in the additive Schwarz method. Note that each contribution from the sum in (3.2) can be computed locally in parallel.

The RAS approach, using the classical choice of Dirichlet transmission conditions, applied as a stand-alone stationary iterative method need not converge since frequencies in the error smaller than the wave number k are not diminished [11]. When used as a preconditioner, the iterative solver used will typically suffer from slow convergence and may stagnate. Further, the local Dirichlet problems involving A_s are not

necessarily well-posed as k^2 may be an eigenvalue of the corresponding Laplace problem, in which case A_s is singular. While methods to handle such singular systems can be applied, a different approach, which provides a convergent stand-alone method, is to change the Dirichlet transmission conditions to Robin conditions. This results in the so-called optimised restricted additive Schwarz (ORAS) method given by

$$(3.3) \quad M_{\text{ORAS}}^{-1} = \sum_{s=1}^N R_s^T D_s \widehat{A}_s^{-1} R_s,$$

where now \widehat{A}_s is the discretisation of the local Robin problem

$$(3.4a) \quad -\Delta w_s - k^2 w_s = f \quad \text{in } \Omega_s,$$

$$(3.4b) \quad \mathcal{C}(w_s) = 0 \quad \text{on } \partial\Omega_s \cap \partial\Omega,$$

$$(3.4c) \quad \frac{\partial w_s}{\partial \mathbf{n}_s} + ikw_s = 0 \quad \text{on } \partial\Omega_s \setminus \partial\Omega,$$

with \mathcal{C} representing the underlying problem boundary conditions on $\partial\Omega$. The local problem (3.4) will always have a unique solution w_s . We note that the use of Robin conditions is not the only remedial choice. Optimal transmission conditions can also be studied and are given using a Dirichlet-to-Neumann (DtN) map [11], however this results in requiring pseudodifferential operators and is somewhat less practical without further approximation. We do not follow the pursuit of more advanced transmission conditions in this work.

The above approaches, RAS and ORAS, are one-level methods: they rely only on local subdomain solves and the local transmission of data. Such domain decomposition methods do not scale as we increase the number of subdomains used; that is, their convergence behaviour depends on N . To achieve robustness with respect to N , a coarse space is typically included, giving a two-level method. The coarse space is represented by a collection of column vectors Z , having full column rank. A coarse space operator $E = Z^\dagger A Z$ is constructed as well as the coarse correction operator $Q = Z E^{-1} Z^\dagger$; note the similarity to terms in (3.2). The inclusion of the coarse space can be done in a number of ways, the simplest being additively as

$$(3.5) \quad M_{2\text{-level}}^{-1} = M_{1\text{-level}}^{-1} + Q,$$

where $M_{1\text{-level}}^{-1}$ is the underlying one-level preconditioner used, such as (3.2) or (3.3). Hybrid approaches are often more effective and we shall consider the adapted deflation technique

$$(3.6) \quad M_{2\text{-level}}^{-1} = M_{1\text{-level}}^{-1} P + Q = M_{1\text{-level}}^{-1} (I - A Q) + Q,$$

where $P = I - A Q$ is a projection. The most crucial choice is that of Z , which provides the coarse space. This is what we shall now consider.

4. Coarse spaces. The construction of a suitable coarse space can be achieved in different ways. A natural approach is to utilise a coarse grid in order to approximate the global behaviour. Often, the slow convergence in the one-level method can be characterised by “slow modes” which should be incorporated into the coarse space. For instance, in the Poisson problem slow modes correspond to constant functions in the kernel of the Laplace operator in each subdomain and these are used to give the

Nicolaides coarse space. On the other hand, for homogeneous elasticity problems the slow modes are rigid body motions.

The notion that certain modes are responsible for slow convergence and must be incorporated into the coarse space can be made more general, in particular in the framework of spectral coarse spaces. Such coarse spaces use spectral information from an appropriate eigenproblem to identify relevant modes that should feature in the coarse space. Before considering spectral coarse spaces we first outline the grid coarse space.

Remark 4.1 (Notation). Following on from [Section 3](#), for a variational problem giving rise to a system matrix B we denote by B_s the corresponding local Dirichlet matrix on Ω_s . Where Robin conditions are used on internal subdomain interfaces (the artificial boundaries) the local problem matrix is denoted by \widehat{B}_s . Meanwhile, when Neumann conditions are used on such interfaces, the local matrix is denoted by \widetilde{B}_s .

4.1. The grid coarse space method. The grid coarse space was first introduced in [\[23\]](#) for the absorptive Helmholtz problem and extended to incorporate impedance (or Robin) conditions in [\[26\]](#). In this case the one-level method is based on the following formula

$$(4.1) \quad M_{1,\varepsilon}^{-1} = \sum_{s=1}^N R_s^T D_s \widehat{A}_{s,\varepsilon}^{-1} R_s.$$

where matrices $\widehat{A}_{s,\varepsilon}$ stem from the discretisation of the following local Robin problems with absorption (given by the parameter $\varepsilon \neq 0$)

$$\begin{aligned} -\Delta u_s - (k^2 + i\varepsilon)u_s &= f && \text{in } \Omega_s, \\ \mathcal{C}(u_s) &= 0 && \text{on } \partial\Omega_s \cap \partial\Omega, \\ \frac{\partial u_s}{\partial \mathbf{n}_s} + iku_s &= 0 && \text{on } \partial\Omega_s \setminus \partial\Omega. \end{aligned}$$

In order to achieve weak dependence on the wave number k and number of subdomains N , the two-level preconditioner can be written in a generic way as follows

$$(4.2) \quad M_{2,\varepsilon}^{-1} = M_{1,\varepsilon}^{-1}P + ZE^{-1}Z^\dagger,$$

where $M_{1,\varepsilon}^{-1}$ is the one-level preconditioner [\(4.1\)](#), Z is a rectangular matrix with full column rank, $E = Z^\dagger \widehat{A}_\varepsilon Z$ is the so-called coarse grid matrix, $Q = ZE^{-1}Z^\dagger$ is the so-called coarse grid correction matrix, and $P = I - A_\varepsilon Q$.

Perhaps the most natural coarse space is the one based on a coarser mesh, which we call the ‘‘grid coarse space’’. Let us consider $\mathcal{T}^{H_{\text{coarse}}}$, a simplicial mesh of Ω with mesh diameter H_{coarse} , and $V^{H_{\text{coarse}}} \subset V$, the corresponding finite element space. Let $\mathcal{I}_0: V^{H_{\text{coarse}}} \rightarrow V^h$ be the nodal interpolation operator and define Z as the corresponding matrix. Then, in this case, $E = Z^\dagger \widehat{A}_\varepsilon Z$ is really the stiffness matrix of the problem (with absorption) discretised on the coarse mesh. Related preconditioners without absorption are used in [\[33\]](#).

4.2. The DtN coarse space. The Dirichlet-to-Neumann (DtN) coarse space [\[36, 10\]](#) is based on solving local eigenvalue problems on subdomain boundaries related to the DtN map. To define this map for the Helmholtz problem we first require the Helmholtz extension operator from the boundary of a subdomain Ω_s .

Let $\Gamma_s = \partial\Omega_s \setminus \partial\Omega$ and suppose we have Dirichlet data v_{Γ_s} on Γ_s , then the Helmholtz extension v in Ω_s is defined as the solution of

$$\begin{aligned} (4.3a) \quad & -\Delta v - k^2 v = 0 && \text{in } \Omega_s, \\ (4.3b) \quad & v = v_{\Gamma_s} && \text{on } \Gamma_s, \\ (4.3c) \quad & \mathcal{C}(v) = 0 && \text{on } \partial\Omega_s \cap \partial\Omega, \end{aligned}$$

where $\mathcal{C}(v) = 0$ represents the original problem boundary conditions, as in (1.1b). The DtN map takes in the Dirichlet data v_{Γ_s} on Γ_s and gives as output the corresponding Neumann data, that is

$$(4.4) \quad \text{DtN}_{\Omega_s}(v_{\Gamma_s}) = \left. \frac{\partial v}{\partial \mathbf{n}_s} \right|_{\Gamma_s}$$

where v is the Helmholtz extension defined by (4.3).

We now seek eigenfunctions of the DtN map locally on each subdomain Ω_s , given by solving

$$(4.5) \quad \text{DtN}_{\Omega_s}(u_{\Gamma_s}) = \lambda u_{\Gamma_s}$$

for eigenfunctions u_{Γ_s} and eigenvalues $\lambda \in \mathbb{C}$. To provide functions to go into the coarse space, we take the Helmholtz extension of u_{Γ_s} in Ω_s and then extend by zero into the whole domain Ω using the partition of unity.

To formulate the discrete problem we require the coefficient matrices \tilde{A}_s corresponding to local Neumann problems on Ω_s with boundary conditions $\mathcal{C} = 0$ on $\partial\Omega_s \cap \partial\Omega$, defined analogously to that of the local Robin problems in (3.4). Further, we need to distinguish between degrees of freedom on the boundary Γ_s and the interior of the subdomain Ω_s , as such we let Γ_s and I_s be the set of indices on the boundary and interior respectively. We also let

$$(4.6) \quad M_{\Gamma_s} = \left(\int_{\Gamma_s} \phi_j \phi_i \right)_{i,j \in \Gamma_s}$$

denote the mass matrix on the subdomain interface. Using standard block notation to denote submatrices of A_s and \tilde{A}_s the discrete DtN eigenproblem is

$$(4.7) \quad \left(\tilde{A}_{\Gamma_s, \Gamma_s} - A_{\Gamma_s, I_s} A_{I_s, I_s}^{-1} A_{I_s, \Gamma_s} \right) \mathbf{u}_{\Gamma_s} = \lambda M_{\Gamma_s} \mathbf{u}_{\Gamma_s}.$$

The Helmholtz extension of \mathbf{u}_{Γ_s} to degrees of freedom in I_s is then given by $\mathbf{u}_{I_s} = -A_{I_s, I_s}^{-1} A_{I_s, \Gamma_s} \mathbf{u}_{\Gamma_s}$. Letting \mathbf{u}_s denote the Helmholtz extension, the corresponding vector which enters the coarse space Z is $R_s^T D_s \mathbf{u}_s$. For further details and motivation behind the DtN eigenproblems see [10].

It remains to determine which eigenfunctions of (4.7) should go on to be included in the coarse space. Several selection criteria were investigated in [10] and it was clear that the best choice was to select eigenvectors corresponding to eigenvalues with the smallest real part. That is, we use a threshold on the abscissa $\eta = \text{Re}(\lambda)$ given by

$$(4.8) \quad \eta < \eta_{\max}$$

where η_{\max} depends on $k_s = \max_{\mathbf{x} \in \Omega_s} k(\mathbf{x})$. In particular, the choice $\eta_{\max} = k_s$ is advocated in [10]. Note that for larger η_{\max} more eigenfunctions are included in the

coarse space, increasing its size and the associated computational cost. Nonetheless, it was recently showed that taking a slightly larger threshold $\eta_{\max} = k_s^{4/3}$ can be beneficial in certain cases in order to gain robustness to the wave number [6]. However, this only occurs for the homogeneous problem with sufficiently uniform subdomains. Since it is not necessarily known in advance how many eigenvalues are below the threshold and in order to make a fair comparison in our numerical tests, we will consider using a fixed number of eigenvectors per subdomain.

4.3. The GenEO coarse space. The GenEO (Generalised Eigenproblems in the Overlap) coarse space was derived in [39] to provide a rigorously robust approach for symmetric positive definite problems even in the presence of heterogeneities. The fundamental generalised eigenproblems on Ω_s at the variational level are given by

$$(4.9) \quad a_{\Omega_s}(u, v) = \lambda a_{\Omega_s^\circ}(\Xi_s(u), \Xi_s(v)) \quad \forall v \in V(\Omega_s),$$

where Ξ_s represents the action of the partition of unity on Ω_s and Ω_s° is the overlapping zone, that is the part of Ω_s which overlaps with any other subdomain. Here $a_D(\cdot, \cdot)$ stems from the underlying variational problem on the domain D , in particular with problem boundary conditions on $\partial\Omega$ and natural (Neumann) conditions on parts of ∂D internal to Ω . The particular form of eigenproblem in (4.9) arises naturally in the analysis of [39]. We also note that (4.9) possesses infinite eigenvalues when there exists $u \neq 0$ such that $a_{\Omega_s^\circ}(\Xi_s(u), \Xi_s(v)) = 0 \forall v \in V(\Omega_s)$ but $a_{\Omega_s}(u, v) \neq 0$ for some $v \in V(\Omega_s)$, for example when u is supported only outside Ω_s° .

The discrete form of the eigenproblem (4.9) is

$$(4.10) \quad \tilde{A}_s \mathbf{u} = \lambda D_s \tilde{A}_s^\circ D_s \mathbf{u}$$

where \tilde{A}_s° is the (Neumann) matrix built from assembling only over elements in the overlapping zone Ω_s° . The eigenfunctions selected to enter the coarse space are the low frequency modes, that is those corresponding to the smallest eigenvalues. Typically, either a fixed number of eigenfunctions are taken per subdomain or a threshold $\lambda < \lambda_{\max}$ on the corresponding eigenvalues is used, where λ_{\max} can be chosen based on problem parameters to achieve a specified condition number of the preconditioned system; see [39].

The precise formulation of the eigenproblem and use of the overlapping zone is somewhat flexible. In particular, the overlapping zone can be replaced with the whole subdomain, as in [27] which utilises an eigenproblem of the form

$$(4.11) \quad \tilde{A}_s \mathbf{u} = \lambda D_s A_s D_s \mathbf{u}.$$

It is this form of GenEO that we shall build upon shortly. We note that two separate GenEO eigenproblems can also be formulated to provide bounds on both ends of the preconditioned spectrum, as is found when using an symmetric ORAS approach in [27]. This flexibility and robustness of GenEO-type methods has yet to be fully explored, especially for problems which are not symmetric positive definite where current theory breaks down. We now consider the utility of using GenEO as basis for constructing a coarse space for the heterogeneous Helmholtz problem.

4.4. A GenEO-type coarse space for the Helmholtz equation. In pursuing a GenEO approach for the Helmholtz equation we must first note the matrices \tilde{A}_s and A_s , now stemming from the bilinear form (2.3a), are no longer symmetric positive definite. As such, eigenvalues λ of the eigenproblem (4.11) are no longer real

and positive (or infinite). As a threshold criterion, as with the DtN approach, we can consider the abscissa $\eta = \operatorname{Re}(\lambda)$ instead and seek eigenfunctions corresponding to $\eta < \eta_{\max}$. Further, since the theory breaks down without the symmetric positive definite assumption, it is no longer clear that (4.11) provides appropriate eigenvectors for the coarse space. Indeed, applying out of the box the GenEO method using (4.11) fails to provide a satisfactory method.

Since GenEO is designed for positive definite problems, a natural proposal is to use a nearby positive definite problem in the formulation of the eigenproblem, namely a Laplace problem, that is setting $k = 0$ for the purpose of constructing the coarse space. Let L_s be local Dirichlet matrix corresponding to the discrete Laplacian and \tilde{L}_s the equivalent Neumann matrix on Ω_s , then

$$(4.12) \quad \tilde{L}_s \mathbf{u} = \lambda D_s L_s D_s \mathbf{u}.$$

has positive real eigenvalues. While this approach can perform reasonable well when the wave number k is small, the behaviour as k grows becomes increasingly poor, as might be expected given the coarse space is independent of k .

To incorporate k we instead link the underlying Helmholtz problem to the positive definite Laplace problem to formulate a GenEO-type eigenproblem

$$(4.13) \quad \tilde{A}_s \mathbf{u} = \lambda D_s L_s D_s \mathbf{u}.$$

Eigenvalues of (4.13) are now, in general, complex (though we note they primarily appear to cluster close to the real line) and so we suggest to threshold based on the abscissa $\eta < \eta_{\max}$. We call this GenEO-type approach for the Helmholtz problem ‘‘H-GenEO’’. Some initial exploration of this method can be found in [5], where the approach is seen to perform well for a 2D wave-guide problem and provide robustness to heterogeneity as well as to the wave number k , albeit requiring a comparatively large coarse space. Again, in our numerical experiments we take a fixed number of eigenvectors and vary this amount, aiming to give a relatively fair comparison of the spectral coarse space methods.

5. Implementation details. Numerical results within this paper have been obtained using FreeFEM [28]. More precisely, `ffddm`—a light-weight layer in FreeFEM domain specific language that generates all domain decomposition data structures—was used on top of HPDDM [30], which handles the underlying computations such as matrix–vector products or preconditioner applications. When it comes to spectral two-level methods, as depicted in the previous subsections 4.2 to 4.4, the bulk of the work comes from the local eigensolves, see, e.g., (4.7), (4.10), and (4.13). These are performed concurrently in each subdomain, using solvers such as ARPACK [35] of SLEPc [29]. Then, the construction of the algebraic Galerkin operator Q introduced in section 3 is performed in HPDDM. In order to deal efficiently with both large numbers of subdomains and large numbers of local eigenvectors, the assembly and exact LU factorization of Q is performed on a subset of processes from the global communicator. We use MUMPS [1] both as a subdomain solver and a coarse operator solver in our experiments. Again, we refer interested readers to [30] for more details about this subject.

For the grid coarse space method from subsection 4.1, two meshes of the same domain must be considered simultaneously. First a coarse one, see an example Figure 5.1a, and then a fine one, see examples Figures 5.1b and 5.1c. We generate fine meshes using a uniform refinement in which edges of all triangles or tetrahedra are

divided uniformly in s . In the aforementioned example, $s = 2$. Note that if one wants $n_{\text{ppwl}}h \approx \lambda$ on the fine grid, on which the original algebraic system of equations (2.5) stems from, then the coarse mesh has to satisfy $H_{\text{coarse}} = \frac{h}{s}$. When it comes to the underlying domain decomposition preconditioners, two options will be considered next. One where both levels of overlap on fine and coarse grids are minimal, i.e., 1, see Figure 5.1b, and another where the level of overlap on the coarse grid is minimal, i.e., 1, and where the level of overlap on the fine grid is s , see Figure 5.1c. In the latter case, note that subdomains on the fine grid are merely uniformly refined subdomains of the coarse grid. While the setup cost of such a two-level preconditioner is much lower than for a spectral method as described in the previous paragraph, applying it to a vector, for example in a Krylov method, is usually costlier. Indeed, the coarse problem is in this case often solved iteratively, instead of using an exact factorization of the coarse operator. This outer–inner strategy, which also makes the use of flexible methods such as FGMRES [38] mandatory, may not perform very well prior to some tuning of the inner (coarse) solver.

In the numerical experiments presented in this paper, the inner coarse problem in the grid coarse space method is defined with a splitting level $s = 2$ and is solved approximately with GMRES preconditioned by a one-level method, with a tolerance of 0.1. Additionally, in the spirit of “shifted Laplacian preconditioning” (see [15, 34]), the coarse problem is defined with added absorption in the equation. This improves the convergence of the one-level method, which then requires fewer iterations to reach the prescribed inner tolerance. Two-level domain decomposition preconditioners with added absorption have been proposed in the literature for the Helmholtz [24] and Maxwell [4] equations. The amount of added absorption needs to be chosen carefully: if the amount of added absorption is too small, there is no gain in the convergence of the inner coarse problem. On the other hand, if the amount is too large, the coarse problem becomes a bad approximation of the original problem (without absorption), and the number of outer iterations increases. We choose the additional imaginary term to be proportional to the wave number k as a compromise.

We conclude this section by mentioning that all the spectral preconditioners may be used in PETSc [3] through the PCHPDDM preconditioner [31]. When it comes to the grid coarse space method, we have a custom implementation in HPDDM that handles systems with multiple right-hand sides, which are encountered frequently in wave propagation phenomena [40, 37, 12]. PCMG, the PETSc machinery for geometric multigrid, does not handle such systems as of version 3.14.1.

6. Comparative numerical studies. In this section we compare the domain decomposition preconditioners for several challenging heterogeneous test problems. We include problems in both 2D and 3D and vary different characteristics of the problem to understand how they can affect performance. In particular, we are interested in the behaviour for larger wave numbers and for an increasing number of subdomains within the domain decomposition. We will also consider discretisations with differing number of points per wavelength and will see how this can affect performance of the preconditioners. For the approaches that use a spectral coarse space, we further investigate the choice of how many eigenvectors should be taken per subdomain.

In the results that follow, a tabulated value of $-$ signifies that the particular test instance did not run, typically this is for the smallest problem when trying to solve on too many subdomains. When the maximum number of iterations is reached before convergence, we denote this by \times . Depending on the test problem, the maximum number of iterations is set at either 500 or 1000.

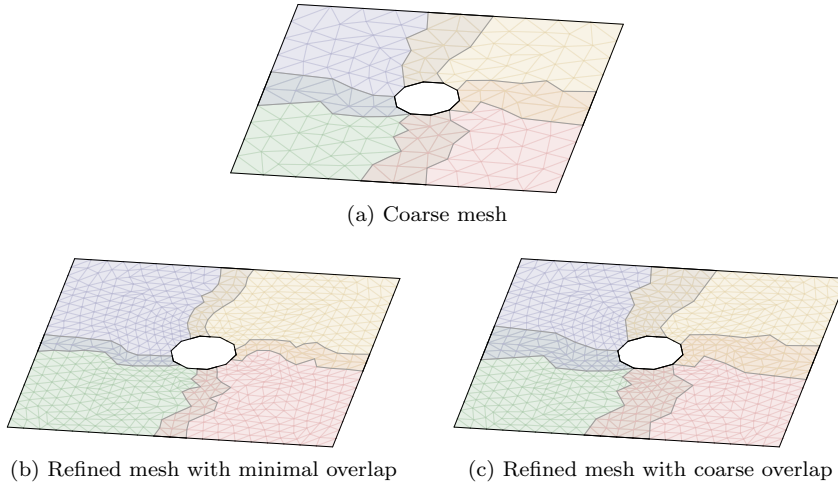


Fig. 5.1: Different overlap definitions (bottom) for a uniformly refined simple 2D coarse mesh (top).

6.1. The Marmousi problem. The Marmousi problem has become a benchmark geophysics test case, consisting of a 2D rectangular domain with velocity data modelling a heterogeneous subsurface. We utilise this as the wave speed within our Helmholtz model with a source of frequency f towards the edge of the domain.

We first consider discretisation with 5 points per wavelength. In Table 6.1 we show results for the one-level method with minimal overlap and also with minimal overlap from the coarse grid (twice the overlap) as references to compare to. Further, Table 6.1 gives results for the two-level coarse grid approach with minimal overlap from the coarse grid. We see that both cases of the one-level method are not scalable (iteration counts increase as the number of subdomains N increases) and perform worse as the frequency f becomes higher. On the other hand, the two-level coarse grid approach is reasonably scalable and with only mildly increasing iteration counts as the frequency increases.

Table 6.1: Results using the one-level and coarse grid methods for the Marmousi problem when using 5 points per wavelength, varying the frequency f and the number of subdomains N .

$f \setminus N$	One-level (min. overlap)					One-level (coarse overlap)					Coarse grid				
	10	20	40	80	160	10	20	40	80	160	10	20	40	80	160
1	30	46	78	98	—	26	39	47	64	—	15	18	19	20	—
5	57	82	117	170	236	53	76	105	154	213	26	29	28	29	31
10	75	111	173	232	330	68	102	158	212	302	32	35	41	40	42
20	89	133	193	268	373	82	125	178	248	347	34	35	42	43	44

We now turn to the two spectral coarse space methods with results in Table 6.2 being given for varying number of eigenvectors taken per subdomain ν . We first see that the H-GenEO method within this scenario performs poorly and, without suffi-

ciently many eigenvectors being taken, often exhibits iteration counts worse than the one-level method. On the other hand, the DtN method generally converges faster than the one-level method and, with enough eigenvectors, can give reasonable performance. However, as the frequency increases the approach begins to struggle a little with larger iteration counts typically required for convergence even with more eigenvectors being utilised. Nonetheless, for small frequencies the approach can beat the coarse grid method with relatively few eigenvectors per subdomain and even for the larger frequency tested, when using the most subdomains and sufficient eigenvectors per subdomain the DtN approach converges faster than the coarse grid method. We note by way of caution though that taking too many eigenvectors per subdomain can eventually lead to some deterioration in the performance of the DtN method. We can also see from [Table 6.2](#) that the larger coarse overlap is beneficial for the DtN method and primarily yields smaller iterations counts. On the other hand, minimal overlap appears preferable for H-GenEO.

Overall, while the DtN approach can reduce the number of iterations required for convergence compared to the coarse grid method in some cases, particularly low frequencies, the coarse grid approach exhibits greater robustness and requires relatively low iterations counts, suggesting it is the favourable approach in this scenario of using 5 points per wavelength.

We now consider the case of discretisation with 10 points per wavelength and similarly compare the different approaches. In [Table 6.3](#) we show results for the one-level methods along with the coarse grid method. We notice that the iteration counts in this situation are slightly higher than when using 5 points per wavelength but otherwise the picture remains similar with coarse grid approach giving a reasonably robust method albeit with some slow growth in iteration counts as the frequency is increased.

Turning to the spectral coarse space approaches, we see in [Table 6.4](#) that H-GenEO now becomes competitive. For larger frequencies and equivalent numbers of eigenvectors taken per subdomain, the H-GenEO method generally requires fewer iterations and this is particularly true for the large frequencies with many subdomains. We note that the minimal overlap case is preferable for H-GenEO while for DtN there is no longer a clear-cut preference between the coarse overlap and minimal overlap cases. Provided sufficiently many eigenvectors are taken per subdomain, we see that H-GenEO now outperforms the coarse grid approach in terms of iterations counts and is particularly strong for the large frequency and many subdomain situation.

Overall, in the scenario of 10 points per wavelength, we have different finding from the 5 point per wavelength scenario. Now, while the coarse grid approach is still relatively robust, the H-GenEO method can be seen as strong alternative which is able to markedly reduce the number of iterations required in the case of large frequencies and many subdomains.

6.2. The COBRA cavity. The COBRA cavity problem consists of a plane wave incidence upon a curving cavity aperture and scattering in 3D. The geometry is shown in [Figure 6.1](#).

We consider discretisation of the problem with 5 points per wavelength using P2 finite elements. In [Table 6.5](#) we display results for the underlying one-level method and the two-level coarse grid approach. The one-level method performs poorly as expected, however, we also see that the coarse grid approach lacks robustness in this setting and performs poorly for larger wave numbers.

Comparing now the spectral coarse space methods, in [Table 6.6](#) we observe that,

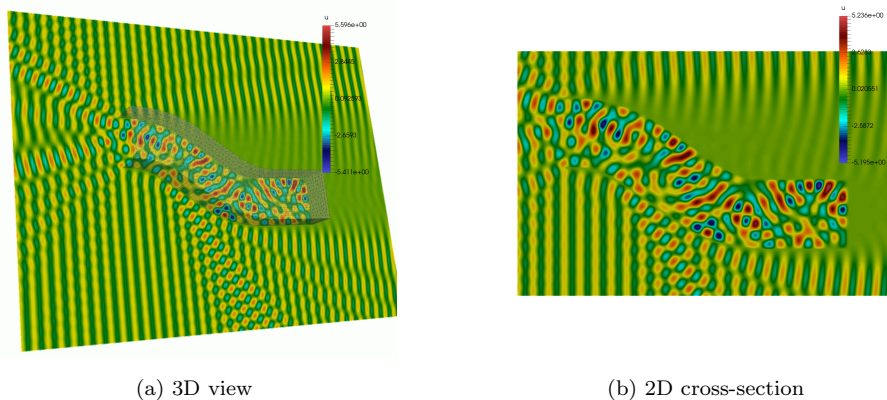


Fig. 6.1: The COBRA cavity problem

in this scenario, the H-GenEO method performs poorly and is often worse than the one-level method, even when taking fairly large numbers of eigenvectors per subdomain. The DtN method can also perform worse than the one-level method in some cases without sufficiently many eigenvectors being taken. However, the DtN approach begins to show relatively low iteration counts once enough eigenvectors are utilised, especially in the many subdomain cases, and can significantly reduce the iteration counts compared to the one-level or coarse grid approaches. Nonetheless, it appears for this 3D problem that the number of eigenvectors required in order to drive down the overall iteration count is rather high.

We also consider the case of discretising the problem with 10 points per wavelength, again using P2 finite elements. Results in Table 6.7 show that in this case the coarse grid method performs very well and consistently leads to a small number of iterations being required for convergence; this is in stark contrast to the 5 points per wave case. For the spectral coarse spaces, as detailed in Table 6.8, the H-GenEO method remains poor, especially for large wave numbers, while the DtN method can perform reasonably well when enough eigenvectors are employed, but in this case not strongly enough to compete in line with the coarse grid method.

6.2.1. The COBRA cavity in 2D. While the COBRA cavity is a 3D problem, we can additionally consider a 2D cross section, as illustrated in Figure 6.1b, and formulate the problem on such a slice. This allows us to consider at a cavity problem in 2D and further consider higher wave numbers.

Results for this 2D COBRA cavity problem at 5 points per wavelength are given in Tables 6.9 and 6.10. Similarly to the full 3D problem, we see that the coarse grid method again lacks robustness in this scenario as the wave number k increases and the H-GenEO is unable to provide any benefit over the one-level method. The DtN is able to provide the lowest iteration counts and for relatively few eigenvectors per subdomain, indeed, it appears that asking for more eigenvectors can become counterproductive here, which may hint that the underlying eigensolvers begin to struggle.

The case of 10 points per wavelength is covered in Tables 6.11 and 6.12 and, again, we broadly see a picture akin to the full 3D problem. In this setting the coarse grid

approach provides good performance and the DtN method also yield low iteration counts when sufficiently many eigenvectors are taken.

6.3. The Overthrust problem. We will now assess our methods on the 3D $20 \times 20 \times 4.65$ km SEG/EAGE Overthrust model introduced by Aminzadeh et al. in 1997. We use a homogeneous Dirichlet boundary condition at the surface and first-order absorbing boundary conditions along the other five faces of the model. The source is located at $(2.5, 2.5, 0.58)$ km and we perform a simulation with P2 finite elements tetrahedral meshes for the 0.5 Hz, 1 Hz and 2Hz frequencies. For higher frequencies and large scale computations on the Overthrust problem by using the grid coarse space see [12] and [13].

We will start by testing the one-level and coarse grid methods when using 5 points per wavelength, varying the frequency f and the number of subdomains N . Results are shown in Table 6.13 and then for the H-GenEO and DtN spectral coarse space methods when using 5 points per wavelength, varying the frequency f , the number of subdomains N , and the number of eigenvectors used per subdomain ν , in Table 6.14. We see that in the case of lower frequency and low resolution the grid coarse space proves to be robust.

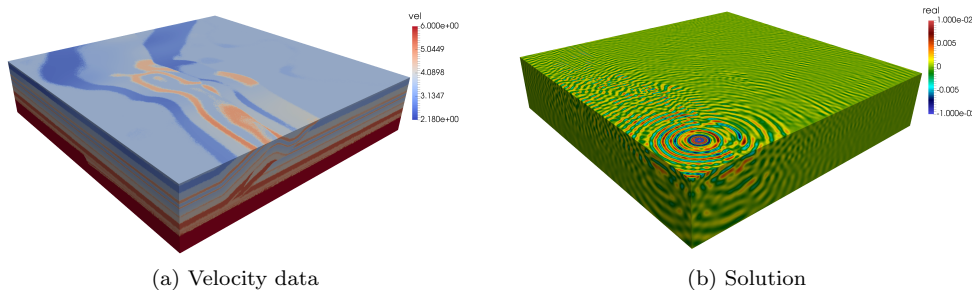


Fig. 6.2: The Overthrust problem

We now increase the frequency to $f = 5$ Hz while keeping the resolution low. The number of degrees of freedom in this case is more significant than before, i.e. 21935538, and for this reason we use a higher number of subdomains. Results with the grid coarse space in Table 6.15 show that this method is performing well in this case whereas the spectral methods are not converging within 500 iterations, as detailed in Table 6.16.

We move on to a higher resolution of 10 points per wavelength for $f = 2$ Hz, varying the number of subdomains N . The number of degrees of freedom is now 11334869. Results for the grid coarse space, in Table 6.17, and for spectral coarse spaces, in Table 6.18, show again that the grid coarse space performs very well but the DtN method now seems to be more stable than before. For reference, we also report in parentheses the average number of inner iterations for solving the coarse problem when using the grid coarse space.

The final tests are performed for $f = 5$ Hz and 2560 subdomains. The number of degrees of freedom is 174352724. The coarse grid method performs again very well, as seen in Table 6.19 whereas the spectral methods experience some difficulties, especially when we increase the number of eigenvectors per domain, as detailed in Table 6.20.

6.4. Discussion of numerical results. Numerical assessment of the three coarse spaces considered shows that, depending on the physical parameters (low or high frequency) or on the resolution considered (low or high resolution), there is no systematic advantage of one method over another, as shown in the overview in Table 6.21. The underlying problem characteristics can play a strong role in the performance of each of these methods and each method has potential tuning parameters that can affect their efficacy, such as the splitting parameter s for the grid coarse space, or the number of eigenvectors requested for the spectral coarse spaces. Further, in situations with multiple right-hand sides the additional precomputation required by the spectral coarse spaces becomes less of a burden compared to the inner iterations required to solve the coarse problems when using the grid coarse space.

Nonetheless, we can provide some general observations from our numerical tests. The coarse grid approach is overall fairly robust in terms of the outer iteration counts required and for high wave numbers, so long as enough points per wavelength or used for discretisation. This method tended to be most favourable in the 10 points per wavelength scenarios. The H-GenEO approach, while able to give some positive results for the geophysical test cases at sufficient resolution, failed to be robust for the cavity problems tested, suggesting it may only be a suitable solver method for certain types of problems. The DtN approach performed relatively well in our tests so long as sufficiently many eigenvectors were utilised and, in particular, tended to be the favourable method in the 5 points per wavelength scenarios. Nonetheless, for the large 3D geophysical test the method struggled somewhat and ultimately becomes somewhat memory demanding if many eigenvectors are to be computed.

7. Conclusions. Tests on these well-known benchmark problems can be further improved and the conclusion refined. We have not measured timings or considered optimised implementations of eigenvalue problems and, in the case of the grid coarse space, the coarse grid is the finest possible which further requires another domain decomposition method to solve it as an inner iteration.

REFERENCES

- [1] P. Amestoy, I. Duff, J.-Y. L'Excellent, and J. Koster. A fully asynchronous multifrontal solver using distributed dynamic scheduling. *SIAM Journal on Matrix Analysis and Applications*, 23(1):15–41, 2001.
- [2] I. M. Babuska and S. A. Sauter. Is the pollution effect of the FEM avoidable for the Helmholtz equation considering high wave numbers? *SIAM Journal on Numerical Analysis*, 34(6):2392–2423, 1997.
- [3] S. Balay, S. Abhyankar, M. F. Adams, J. Brown, P. Brune, K. Buschelman, L. Dalcin, A. Dener, V. Eijkhout, W. D. Gropp, D. Karpeyev, D. Kaushik, M. G. Knepley, D. A. May, L. C. McInnes, R. T. Mills, T. Munson, K. Rupp, P. Sanan, B. F. Smith, S. Zampini, H. Zhang, and H. Zhang. PETSc users manual. Technical Report ANL-95/11 - Revision 3.13, Argonne National Laboratory, 2020.
- [4] M. Bonazzoli, V. Dolean, I. G. Graham, E. A. Spence, and P.-H. Tournier. Domain decomposition preconditioning for the high-frequency time-harmonic maxwell equations with absorption. *Math. Comp.*, 88:2559–2604, 2019.
- [5] N. Bootland. Coarse spaces for Helmholtz. In *Scottish Numerical Methods Network Workshop on Iterative Methods for Partial Differential Equations*, available online at <http://personal.strath.ac.uk/jennifer.pestana/lms19/Bootland.pdf>, 27 September 2019.
- [6] N. Bootland and V. Dolean. On the Dirichlet-to-Neumann coarse space for solving the Helmholtz problem using domain decomposition. In *European Conference on Numerical Mathematics and Advanced Applications*. Springer, 2019.
- [7] A. Brandt and I. Livshits. Wave-ray multigrid method for standing wave equations. *Electron. Trans. Numer. Anal.*, 6:162–181, 1997.
- [8] P. Chevalier and F. Nataf. Symmetrized method with optimized second-order conditions for the

- Helmholtz equation. In *Domain decomposition methods, 10 (Boulder, CO, 1997)*, pages 400–407. Amer. Math. Soc., Providence, RI, 1998.
- [9] F. Collino, G. Delbue, P. Joly, and A. Piacentini. A new interface condition in the non-overlapping domain decomposition for the Maxwell equations Helmholtz equation and related optimal control. *Comput. Methods Appl. Mech. Engrg.*, 148:195–207, 1997.
 - [10] L. Conen, V. Dolean, R. Krause, and F. Nataf. A coarse space for heterogeneous Helmholtz problems based on the Dirichlet-to-Neumann operator. *J. Comput. Appl. Math.*, 271:83–99, 2014.
 - [11] V. Dolean, P. Jolivet, and F. Nataf. *An introduction to domain decomposition methods*. Society for Industrial and Applied Mathematics (SIAM), Philadelphia, PA, 2015. Algorithms, theory, and parallel implementation.
 - [12] V. Dolean, P. Jolivet, P.-H. Tournier, and S. Operto. Iterative frequency-domain seismic wave solvers based on multi-level domain-decomposition preconditioners. In *82th Annual EAGE Meeting (Amsterdam)*, volume arXiv:2004.06309, 2020.
 - [13] V. Dolean, P. Jolivet, P.-H. Tournier, and S. Operto. Large-scale frequency-domain seismic wave modeling on h -adaptive tetrahedral meshes with iterative solver and multi-level domain-decomposition preconditioners. In *SEG2020 Annual Meeting*, 2020. arXiv:2004.07930.
 - [14] V. Dolean, F. Nataf, R. Scheichl, and N. Spillane. Analysis of a two-level Schwarz method with coarse spaces based on local Dirichlet-to-Neumann maps. *Comput. Methods Appl. Math.*, 12(4):391–414, 2012.
 - [15] Y. A. Erlangga, C. Vuik, and C. W. Oosterlee. On a class of preconditioners for solving the Helmholtz equation. *Appl. Numer. Math.*, 50(3-4):409–425, 2004.
 - [16] O. G. Ernst and M. J. Gander. Why it is difficult to solve Helmholtz problems with classical iterative methods. In I. G. Graham, T. Y. Hou, O. Lakkis, and R. Scheichl, editors, *Numerical Analysis of Multiscale Problems*, pages 325–363. Springer, 2012.
 - [17] C. Farhat, P. Avery, R. Tezaur, and J. Li. FETI-DPH: a dual-primal domain decomposition method for acoustic scattering. *Journal of Computational Acoustics*, 13(3):499–524, 2005.
 - [18] C. Farhat, A. Macedo, and M. Lesoinne. A two-level domain decomposition method for the iterative solution of high frequency exterior Helmholtz problems. *Numerische Mathematik*, 85(2):283–308, 2000.
 - [19] J. Fish and Y. Qu. Global-basis two-level method for indefinite systems. Part 1: convergence studies. *Internat. J. Numer. Methods Engrg.*, 49(3):439–460, 2000.
 - [20] M. J. Gander, F. Magoulès, and F. Nataf. Optimized Schwarz methods without overlap for the Helmholtz equation. *SIAM J. Sci. Comput.*, 24(1):38–60, 2002.
 - [21] M. J. Gander and H. Zhang. A class of iterative solvers for the Helmholtz equation: Factorizations, sweeping preconditioners, source transfer, single layer potentials, polarized traces, and optimized Schwarz methods. *SIAM Review*, 61(1):3–76, 2019.
 - [22] S. Gong, I. G. Graham, and E. A. Spence. Domain decomposition preconditioners for high-order discretisations of the heterogeneous Helmholtz equation. *arXiv:2004.03996*, 2020.
 - [23] I. G. Graham, E. A. Spence, and E. Vainikko. Domain decomposition preconditioning for high-frequency Helmholtz problems with absorption. *Math. Comp.*, 86(307):2089–2127, 2017.
 - [24] I. G. Graham, E. A. Spence, and E. Vainikko. Domain decomposition preconditioning for high-frequency Helmholtz problems with absorption. *Math. Comp.*, 86(307):2089–2127, 2017.
 - [25] I. G. Graham, E. A. Spence, and E. Vainikko. Recent results on domain decomposition preconditioning for the high-frequency Helmholtz equation using absorption. *Lahaye D., Tang J., Vuik K. (eds) Modern Solvers for Helmholtz Problems. Geosystems Mathematics. Birkhäuser, Cham*, pages 3–26, 2017.
 - [26] I. G. Graham, E. A. Spence, and J. Zou. Domain decomposition with local impedance conditions for the Helmholtz equation. *arXiv:1806.03731*, 2018.
 - [27] R. Haferssas, P. Jolivet, and F. Nataf. An additive Schwarz method type theory for Lions’s algorithm and a symmetrized optimized restricted additive Schwarz method. *SIAM J. Sci. Comput.*, 39(4):A1345–A1365, 2017.
 - [28] F. Hecht. New development in FreeFem++. *Journal of Numerical Mathematics*, 20(3-4):251–266, 2012.
 - [29] V. Hernandez, J. E. Roman, and V. Vidal. SLEPc: A scalable and flexible toolkit for the solution of eigenvalue problems. *ACM Transactions on Mathematical Software*, 31(3):351–362, 2005.
 - [30] P. Jolivet, F. Hecht, F. Nataf, and C. Prud’homme. Scalable domain decomposition preconditioners for heterogeneous elliptic problems. In *Proceedings of the 2013 International Conference on High Performance Computing, Networking, Storage and Analysis*, SC13,

- pages 80:1–80:11. ACM, 2013.
- [31] P. Jolivet, J. E. Roman, and S. Zampini. KSPHPDDM and PCHPDDM: Extending PETSc with robust overlapping Schwarz preconditioners and advanced Krylov methods. *submitted for publication*, 2020.
 - [32] A. Jouadé and A. Barka. Massively parallel implementation of FETI-2LM methods for the simulation of the sparse receiving array evolution of the GRAVES radar system for space surveillance and tracking. *IEEE Access*, 7:128968–128979, 2019.
 - [33] J.-H. Kimn and M. Sarkis. Restricted overlapping balancing domain decomposition methods and restricted coarse problems for the Helmholtz problem. *Computer Methods in Applied Mechanics and Engineering*, 196(8):1507 – 1514, 2007. Domain Decomposition Methods: recent advances and new challenges in engineering.
 - [34] D. Lahaye, J. Tang, and K. Vuik. *Modern solvers for Helmholtz problems*. Springer, 2017.
 - [35] R. Lehoucq, D. Sorensen, and C. Yang. *ARPACK users' guide: solution of large-scale eigenvalue problems with implicitly restarted Arnoldi methods*, volume 6. Society for Industrial and Applied Mathematics, 1998.
 - [36] F. Nataf, H. Xiang, V. Dolean, and N. Spillane. A coarse space construction based on local Dirichlet-to-Neumann maps. *SIAM J. Sci. Comput.*, 33(4):1623–1642, 2011.
 - [37] F.-X. Roux and A. Barka. Block Krylov recycling algorithms for FETI-2LM applied to 3D electromagnetic wave scattering and radiation. *IEEE Transactions on Antennas and Propagation*, 65(4):1886–1895, 2017.
 - [38] Y. Saad. A flexible inner-outer preconditioned GMRES algorithm. *SIAM Journal on Scientific Computing*, 14(2):461–469, 1993.
 - [39] N. Spillane, V. Dolean, P. Hauret, F. Nataf, C. Pechstein, and R. Scheichl. Abstract robust coarse spaces for systems of PDEs via generalized eigenproblems in the overlaps. *Numer. Math.*, 126(4):741–770, 2014.
 - [40] P.-H. Tournier, I. Aliferis, M. Bonazzoli, M. de Buhan, M. Darbas, V. Dolean, F. Hecht, P. Jolivet, I. El Kanfoud, C. Migliaccio, F. Nataf, C. Pichot, and S. Semenov. Microwave tomographic imaging of cerebrovascular accidents by using high-performance computing. *Parallel Computing*, 85:88–97, 2019.

Table 6.2: Results using the H-GenEO and DtN spectral coarse space methods for the Marmousi problem when using 5 points per wavelength, varying the frequency f , the number of subdomains N , and the number of eigenvectors used per subdomain ν .

ν	$f \setminus N$	H-GenEO (min. overlap)					DtN (min. overlap)					H-GenEO (coarse overlap)					DtN (coarse overlap)				
		10	20	40	80	160	10	20	40	80	160	10	20	40	80	160	10	20	40	80	160
20	1	9	14	21	21	—	5	9	6	6	—	16	22	31	34	—	4	5	4	4	—
	5	46	53	67	76	100	36	49	62	71	85	58	86	120	158	201	39	55	71	79	67
	10	67	99	146	173	209	57	85	117	147	196	76	133	220	301	420	59	86	129	177	257
	20	81	120	169	248	378	77	113	156	206	279	83	125	226	370	×	76	115	156	211	297
40	1	9	13	16	21	—	8	11	6	6	—	16	22	26	32	—	6	7	7	5	—
	5	31	32	42	49	71	23	32	37	41	45	46	74	104	137	186	26	32	23	10	6
	10	66	85	105	106	126	46	66	90	106	117	100	153	233	269	373	47	80	110	126	100
	20	86	136	209	264	323	69	102	141	180	249	119	232	391	×	×	70	106	150	222	357
80	1	9	12	18	21	—	5	6	5	6	—	15	20	22	33	—	4	4	5	5	—
	5	20	20	28	41	62	13	22	17	37	61	40	62	87	127	184	9	10	7	14	22
	10	47	56	64	72	88	30	41	46	49	43	88	118	171	225	327	34	40	40	17	13
	20	87	125	171	186	217	58	86	111	147	156	153	246	404	×	×	60	106	159	183	150
160	1	9	11	17	21	—	8	8	5	6	—	16	15	21	33	—	5	6	9	6	—
	5	15	17	26	37	56	11	26	29	22	44	37	59	82	116	171	8	15	9	6	20
	10	33	40	45	56	73	21	24	30	53	84	68	94	143	196	284	20	15	17	34	26
	20	64	83	121	134	157	36	52	70	78	77	131	192	320	403	×	45	66	78	52	38

Table 6.3: Results using the one-level and coarse grid methods for the Marmousi problem when using 10 points per wavelength, varying the frequency f and the number of subdomains N .

$f \setminus N$	One-level (min. overlap)					One-level (coarse overlap)					Coarse grid				
	10	20	40	80	160	10	20	40	80	160	10	20	40	80	160
1	34	49	72	143	–	30	43	63	97	–	16	18	19	21	–
5	62	94	137	191	268	58	87	126	175	246	29	29	34	34	36
10	85	136	185	272	371	78	124	172	251	346	35	41	43	46	45
20	101	152	213	299	419	92	142	198	272	389	39	47	48	49	49

Table 6.4: Results using the H-GenEO and DtN spectral coarse space methods for the Marmousi problem when using 10 points per wavelength, varying the frequency f , the number of subdomains N , and the number of eigenvectors used per subdomain ν .

ν	$f \setminus N$	H-GenEO (min. overlap)					DtN (min. overlap)					H-GenEO (coarse overlap)					DtN (coarse overlap)				
		10	20	40	80	160	10	20	40	80	160	10	20	40	80	160	10	20	40	80	160
20	1	8	8	9	15	—	8	8	5	7	—	7	7	9	14	—	5	6	4	4	—
	5	42	42	39	32	19	42	49	59	51	56	40	46	47	38	32	39	49	67	72	85
	10	78	112	125	133	99	70	105	128	157	166	72	108	133	156	138	65	99	128	169	197
	20	96	136	180	259	342	92	131	175	232	318	89	130	177	248	345	85	125	170	227	315
40	1	7	8	9	14	—	6	5	6	6	—	7	7	9	13	—	4	3	3	4	—
	5	22	19	17	13	14	25	29	31	32	33	21	20	19	17	20	25	34	43	40	38
	10	58	63	54	42	26	49	71	74	84	82	58	70	65	61	44	48	75	88	112	128
	20	101	148	169	161	148	85	120	159	190	217	94	141	183	203	214	80	116	154	194	256
80	1	7	8	9	13	—	7	7	5	5	—	6	7	9	12	—	5	4	3	4	—
	5	13	12	11	10	12	16	16	19	17	10	12	11	12	13	17	19	15	14	7	6
	10	31	28	23	17	15	28	39	40	42	41	30	31	27	23	24	29	47	55	66	34
	20	81	90	78	53	39	63	89	93	100	107	85	104	107	89	69	64	93	108	147	202
160	1	7	8	8	13	—	4	7	5	6	—	6	7	8	11	—	3	6	3	5	—
	5	10	9	10	10	12	10	11	12	17	24	8	9	10	13	16	10	9	8	21	14
	10	20	16	14	13	13	19	23	25	25	24	18	15	16	16	19	21	29	30	25	17
	20	45	40	34	25	19	35	46	47	56	59	50	52	50	39	28	36	61	77	84	76

Table 6.5: Results using the one-level and coarse grid methods for the COBRA cavity problem when using 5 points per wavelength, varying the wave number k and the number of subdomains N .

$k \setminus N$	One-level				Coarse grid			
	20	40	80	160	20	40	80	160
100	71	83	104	–	21	21	22	–
200	161	203	259	303	87	90	91	91
300	326	429	574	727	277	309	330	562
400	326	426	581	705	375	450	463	471

Table 6.6: Results using the H-GenEO and DtN spectral coarse space methods for the COBRA cavity problem when using 5 points per wavelength, varying the wave number k , the number of subdomains N , and the number of eigenvectors used per subdomain ν .

ν	$k \setminus N$	H-GenEO				DtN			
		20	40	80	160	20	40	80	160
20	100	66	86	107	–	47	58	74	–
	200	165	214	284	366	154	199	250	324
	300	334	453	611	809	326	429	569	742
	400	342	440	624	810	337	425	582	727
40	100	65	85	108	–	32	34	28	–
	200	164	216	291	377	145	187	233	262
	300	348	468	638	852	319	424	567	768
	400	366	500	716	981	337	438	594	778
80	100	64	85	108	–	16	13	10	–
	200	155	214	285	382	116	132	100	63
	300	345	461	636	845	301	399	542	573
	400	408	558	771	×	335	453	650	918
160	100	63	85	108	–	10	8	9	–
	200	150	210	282	382	46	41	18	14
	300	324	441	617	830	247	263	249	145
	400	417	547	749	×	350	476	576	484
320	100	–	–	–	–	–	–	–	–
	200	145	207	281	383	14	15	12	11
	300	308	422	601	817	101	62	49	31
	400	401	527	730	994	271	233	149	51

Table 6.7: Results using the one-level and coarse grid methods for the COBRA cavity problem when using 10 points per wavelength, varying the wave number k and the number of subdomains N .

$k \setminus N$	One-level				Coarse grid			
	20	40	80	160	20	40	80	160
50	27	38	47	52	8	8	8	9
100	80	103	115	147	11	23	11	11
150	143	181	235	292	16	16	17	17
200	192	268	308	427	15	15	16	16

Table 6.8: Results using the H-GenEO and DtN spectral coarse space methods for the COBRA cavity problem when using 10 points per wavelength, varying the wave number k , the number of subdomains N , and the number of eigenvectors used per subdomain ν .

ν	$k \setminus N$	H-GenEO				DtN			
		20	40	80	160	20	40	80	160
20	50	26	31	41	46	19	22	20	21
	100	73	94	111	130	63	77	87	112
	150	128	171	230	278	120	157	209	244
	200	186	264	315	427	178	246	283	380
40	50	25	31	40	45	13	12	12	11
	100	72	89	109	132	51	58	66	57
	150	129	168	228	279	112	130	181	211
	200	197	279	328	433	163	225	251	330
80	50	24	31	40	44	8	8	11	9
	100	68	89	106	132	29	30	24	19
	150	131	167	224	281	87	101	109	81
	200	200	270	327	428	142	193	218	255
160	50	24	29	40	44	8	8	11	10
	100	65	87	109	132	18	20	18	15
	150	126	164	220	279	51	36	36	32
	200	192	267	324	430	109	135	97	77
320	50	23	30	40	44	8	8	11	11
	100	63	85	107	133	15	16	18	16
	150	119	158	219	279	33	23	26	26
	200	182	246	311	430	57	64	54	49

Table 6.9: Results using the one-level and coarse grid methods for the 2D COBRA cavity problem when using 5 points per wavelength, varying the wave number k and the number of subdomains N .

$k \setminus N$	One-level				Coarse grid			
	20	40	80	160	20	40	80	160
200	74	99	122	–	30	30	30	–
400	103	155	211	279	67	69	70	70
600	204	303	429	668	145	155	158	160
800	184	287	392	559	197	214	218	219
1000	188	278	400	551	242	265	269	270

Table 6.10: Results using the H-GenEO and DtN spectral coarse space methods for the 2D COBRA cavity problem when using 5 points per wavelength, varying the wave number k , the number of subdomains N , and the number of eigenvectors used per subdomain ν .

ν	$k \setminus N$	H-GenEO				DtN			
		20	40	80	160	20	40	80	160
20	200	59	85	125	–	24	29	19	–
	400	101	135	202	277	78	87	79	41
	600	177	271	371	531	161	228	254	221
	800	192	293	390	517	179	274	341	371
	1000	213	302	428	597	203	288	415	521
40	200	54	84	121	–	21	25	31	–
	400	94	126	192	271	34	18	34	126
	600	164	240	348	505	84	82	41	54
	800	178	259	356	482	129	152	102	42
	1000	203	275	394	555	166	198	195	104
80	200	53	76	109	–	17	16	21	–
	400	86	120	187	261	41	52	34	22
	600	154	226	331	490	26	54	169	90
	800	164	244	338	466	42	37	92	220
	1000	184	256	370	529	73	41	43	303
160	200	53	68	116	–	24	37	34	–
	400	83	119	183	206	29	42	96	132
	600	146	218	322	480	60	42	50	264
	800	154	228	333	458	76	87	38	49
	1000	177	243	358	520	56	132	86	44
320	200	53	68	116	–	22	39	34	–
	400	81	118	182	206	39	28	75	132
	600	138	211	315	477	49	113	64	188
	800	147	221	326	449	34	67	154	92
	1000	169	233	346	512	49	38	193	189

Table 6.11: Results using the one-level and coarse grid methods for the 2D COBRA cavity problem when using 10 points per wavelength, varying the wave number k and the number of subdomains N .

$k \setminus N$	One-level				Coarse grid			
	20	40	80	160	20	40	80	160
200	85	124	171	239	10	11	11	11
400	137	184	270	356	11	11	12	12
600	253	329	478	705	20	20	20	21
800	203	323	448	611	18	18	18	18
1000	217	316	470	656	19	19	19	19

Table 6.12: Results using the H-GenEO and DtN spectral coarse space methods for the 2D COBRA cavity problem when using 10 points per wavelength, varying the wave number k , the number of subdomains N , and the number of eigenvectors used per subdomain ν .

ν	$k \setminus N$	H-GenEO				DtN			
		20	40	80	160	20	40	80	160
20	200	77	114	159	221	36	42	21	16
	400	136	195	273	367	111	147	172	123
	600	241	332	454	658	208	265	346	434
	800	220	338	485	692	186	282	396	533
	1000	242	363	561	787	202	293	419	608
40	200	75	108	153	220	10	7	9	30
	400	137	187	260	354	66	46	21	13
	600	236	320	439	632	152	167	128	51
	800	221	349	470	673	159	236	270	182
	1000	254	378	545	785	186	269	365	394
80	200	73	104	152	219	15	18	11	10
	400	130	174	256	347	12	9	21	39
	600	220	295	414	590	54	22	12	18
	800	213	329	454	642	88	74	25	15
	1000	256	365	528	727	141	147	84	24
160	200	71	104	148	202	7	13	32	38
	400	121	165	246	342	18	18	12	16
	600	210	282	396	577	19	32	45	19
	800	203	308	435	601	21	23	74	47
	1000	245	344	501	688	37	26	33	137
320	200	69	122	148	204	14	9	16	38
	400	116	158	241	355	8	16	35	17
	600	197	266	375	714	23	16	22	93
	800	192	295	412	579	30	26	18	35
	1000	225	324	464	653	42	56	25	25

Table 6.13: Results using the one-level and coarse grid methods for the Overthrust problem when using 5 points per wavelength, varying the frequency f and the number of subdomains N .

$f \setminus N$	One-level (min. overlap)					One-level (coarse overlap)					Coarse grid				
	10	20	40	80	160	10	20	40	80	160	10	20	40	80	160
0.5	16	21	28	35	–	14	17	20	19	–	9	10	10	10	–
1	27	36	55	62	78	24	30	48	50	62	17	19	23	23	25
2	32	47	64	81	104	27	40	53	68	86	18	22	25	27	28

Table 6.14: Results using the H-GenEO and DtN spectral coarse space methods for the Overthrust problem when using 5 points per wavelength, varying the frequency f , the number of subdomains N , and the number of eigenvectors used per subdomain ν .

ν	$f \setminus N$	H-GenEO (min. overlap)					DtN (min. overlap)					H-GenEO (coarse overlap)					DtN (coarse overlap)				
		10	20	40	80	160	10	20	40	80	160	10	20	40	80	160	10	20	40	80	160
20	0.5	11	14	17	30	—	6	6	7	8	—	12	15	19	19	—	5	5	5	6	—
	1	25	33	47	52	60	21	28	43	45	51	25	34	44	49	56	19	28	42	49	53
	2	33	47	62	78	99	31	45	59	72	89	32	48	74	101	134	28	41	57	70	96
40	0.5	10	12	15	25	—	6	6	7	7	—	12	15	18	19	—	4	4	5	5	—
	1	24	32	44	52	59	17	26	37	41	44	24	34	45	50	56	16	24	37	39	42
	2	34	50	70	104	123	30	42	56	69	87	35	61	87	112	146	28	42	61	77	110
80	0.5	9	11	14	26	—	5	6	7	7	—	12	14	18	18	—	4	4	5	5	—
	1	22	31	44	52	60	14	22	30	39	45	23	33	45	50	56	14	22	36	37	41
	2	38	61	84	111	139	28	40	54	69	92	41	63	91	116	158	27	42	63	82	119
160	0.5	9	11	11	28	—	6	6	7	7	—	12	14	17	19	—	4	4	5	5	—
	1	19	29	44	52	60	14	22	34	42	48	23	33	46	50	56	15	24	37	41	45
	2	36	54	77	107	136	27	41	55	70	91	41	62	90	117	159	26	41	64	83	127

Table 6.15: Results using the one-level and coarse grid methods for the Overthrust problem when using 5 points per wavelength for $f = 5$ Hz, varying the number of subdomains N . The number of degrees of freedom is 21935538.

$f \setminus N$	One-level (min. overlap)			One-level (coarse overlap)			Coarse grid		
	320	640	1280	320	640	1280	320	640	1280
5	170	209	256	139	173	213	28(7)	30(8)	30(11)

Table 6.16: Results using the H-GenEO and DtN spectral coarse space methods for the Overthrust problem when using 5 points per wavelength for $f = 5$ Hz, varying the number of subdomains N and the number of eigenvectors used per subdomain ν . The number of degrees of freedom is 21935538.

$\nu \setminus N$	H-GenEO (min. overlap)			DtN (min. overlap)			H-GenEO (coarse overlap)			DtN (coarse overlap)		
	320	640	1280	320	640	1280	320	640	1280	320	640	1280
40	159	231	−?	153	178	−?	310	−	−?	145	189	−?
80	358	−	−	141	176	375	−	−	−	179	−	−
160	489	−	−	171	−?	−	−	−	435	412	−	−
320	455	−	−	255	−?	−?	−	−	434	318	396	−

Table 6.17: Results using the one-level and coarse grid methods for the Overthrust problem when using 10 points per wavelength for $f = 2$ Hz, varying the number of subdomains N . The number of degrees of freedom is 11334869.

$f \setminus N$	One-level (min. overlap)			One-level (coarse overlap)			Coarse grid		
	320	640	1280	320	640	1280	320	640	1280
2	149	185	226	125	156	189	24(7)	24(9)	23(13)

Table 6.18: Results using the H-GenEO and DtN spectral coarse space methods for the Overthrust problem when using 10 points per wavelength for $f = 2$ Hz, varying the number of subdomains N and the number of eigenvectors used per subdomain ν . The number of degrees of freedom is 11334869.

$\nu \setminus N$	H-GenEO (min. overlap)			DtN (min. overlap)			H-GenEO (coarse overlap)			DtN (coarse overlap)		
	320	640	1280	320	640	1280	320	640	1280	320	640	1280
40	69	73	77	99	110	124	170	209	234	102	131	153
80	29	39	41	75	82	89	149	206	245	98	117	145
160	21	28	−	60	86	127	118	189	249	100	134	158
320	18	−	494	80	105	145	97	281	246	104	134	159

Table 6.19: Results using the one-level and coarse grid methods for the Overthrust problem when using 10 points per wavelength for $f = 5$ Hz and 2560 subdomains. The number of degrees of freedom is 174352724.

	One-level (min. overlap)	One-level (coarse overlap)	Coarse grid
$f \setminus N$	2560	2560	2560
5	365	338	30(15)

Table 6.20: Results using the H-GenEO and DtN spectral coarse space methods for the Overthrust problem when using 10 points per wavelength for $f = 5$ Hz and 2560 subdomains, varying the number of eigenvectors used per subdomain ν . The number of degrees of freedom is 174352724.

	H-GenEO (min. overlap)	DtN (min. overlap)	H-GenEO (coarse overlap)	DtN (coarse overlap)
$\nu \setminus N$	2560	2560	2560	2560
40	-	299	-	264
80	-	429	-	-
160	OOM	OOM	OOM	OOM

Table 6.21: An overview of which coarse spaces perform well in the different problem scenarios tests. A \checkmark indicates that the method performs well, with $\checkmark\checkmark$ indicating this method was most favourable in a particular instance. A \times indicates that a method provided relatively little to no gain over the one-level method.

Problem	d	freq	Coarse grid		H-GenEO		DtN	
			5 ppwl	10 ppwl	5 ppwl	10 ppwl	5 ppwl	10 ppwl
Marmousi	2D	low	\checkmark	\checkmark	\checkmark	\checkmark	$\checkmark\checkmark$	$\checkmark\checkmark$
		high	$\checkmark\checkmark$	\checkmark	\times	$\checkmark\checkmark$	\checkmark	\checkmark
COBRA Cavity	2D	low	\checkmark	$\checkmark\checkmark$	\times	\times	$\checkmark\checkmark$	\checkmark
		high	\times	$\checkmark\checkmark$	\times	\times	$\checkmark\checkmark$	\checkmark
COBRA Cavity	3D	low	\checkmark	$\checkmark\checkmark$	\times	\times	$\checkmark\checkmark$	\checkmark
		high	\times	$\checkmark\checkmark$	\times	\times	$\checkmark\checkmark$	\checkmark
Overthrust	3D	low	$\checkmark\checkmark$	$\checkmark\checkmark$	\times	\checkmark	\checkmark	\times
		high	$\checkmark\checkmark$	$\checkmark\checkmark$	\times	\times	\times	\times